A Theoretical Examination of the Electronic Structure and Spectroscopy of the Photosynthetic Reaction Center from *Rhodopseudomonas viridis*

Mark A. Thompson*,† and Michael C. Zerner*

Contribution from the Quantum Theory Project, Department of Chemistry, University of Florida, Gainesville, Florida 32611. *Received December 24, 1990*

Abstract: We report electronic structure calculations of the excited states of a model of the photosynthetic reaction center (RC) from the photosynthetic bacterium *Rhodopseudomonas viridis*. These calculations are performed using the intermediate neglect of differential overlap model (INDO/S) and include the effect of the polarizable protein by utilizing the self-consistent reaction field (SCRF) solvent model. These calculations reproduce the main characteristics of the experimental optical spectra. We are able to identify the two lowest excited states as the lower $P^*_{(-)}$ and upper $P^*_{(+)}$ exciton states of the bacteriochlorophyll *b* (BChlb) dimer (P) separated by about 1300 cm^{-1}, as well as several charge-transfer (CT) states. In both the gas-phase and solvent calculations, the charge-transfer (CT) states on the photoactive L branch are lower than the corresponding CT bands for the M branch. Without including the relaxation that results from the polarization of the media, the CT states are predicted to be some 8000 cm^{-1} higher in energy than the lowest excited state of the BChlb dimer ($P^*_{(-)}$). Including the effects of the protein, even in an averaged way, dramatically lowers the energy of all the CT states. $P^+H_L^-$, the state responsible for the observed charge separation, where H_L designates the bacteriopheophytin *b* on the L branch, is the lowest CT state with a calculated energy only 1200 cm^{-1} above the lowest excitonic state $P^*_{(-)}$, and we argue that geometric relaxation of the RC or of the surrounding protein would lower this CT state even further. These calculations demonstrate the preference for CT along the L branch as well as supplying a rationale for the absence of an explicit intermediate involving the auxiliary BChlb (B_L) that lies between P and H_L in the structure of the RC.

Introduction

The initial events of photosynthesis involve a light-driven separation of charge across the photosynthetic membrane.[1-6] The X-ray crystal structure of the reaction center (RC) of *Rps. viridis* has recently been reported at 2.3-Å resolution.[7] The RC contains four bacteriochlorophyll *b* (BChlb) and two bacteriopheophytin *b* (BPhb) chromophores. In addition there are two quinones (Q_A and Q_B) and a nonheme Fe.[7] Two molecules of BChlb are closely juxtaposed with their pyrrole rings I overlapping at an average macrocycle separation of ~3.3 Å and form the "special pair" or primary donor, hereafter referred to as P, and shown in Figure 1. The remaining chromophores form two branches, each consisting of an auxiliary BChlb, a BPhb, and a quinone. The chromophores of P and the two branches are related by a pseudo-C_2 symmetry axis that extends from P to the nonheme Fe. The monomer subunits of P and the branches are labeled L or M according to their association with either the L or M protein subunits of the RC complex. X-ray crystal structures of the RC from *Rhodobacter sphaeroides* have also been solved to 3.1 Å.[8,9] These RCs contain BChl-a in place of BChlb and exhibit slightly different optical absorbance and electron-transfer rate constants[10-12] but generally are structurally and functionally analogous to the RC of *Rps. viridis*.

The BChlb dimer, P, absorbs excitation energy, either directly or through energy transfer from nearby antennae complexes, and rapidly transfers an electron to the BPhb on the L branch (H_L) in about 3 ps at room temperature.[1-6] This initial charge separation is followed by two slower electron-transfer steps, first to a nearby quinone, Q_A, on the L branch and then to a quinone on the M branch, Q_B.[1-6] Despite the pseudo-2-fold symmetry of the RC, charge separation proceeds only along the L branch.[13] The reasons for this asymmetry are not well understood.

To understand the photophysical properties of bacterial photosynthetic reaction centers (RC) and the process of light-driven electron transfer, we must address the properties of the chromophores as an aggregate as well as their interactions with the surrounding protein. The chromophores in the RC of *Rps. viridis* are shown in Figure 1. In this figure, the phytyl tails of the BChlb's and BPhb's have been truncated for clarity, as have the chelating ligands to the Fe atom. The surrounding protein acts noncovalently as a scaffold to maintain the relative orientations of these chromophores. To perform a quantum chemical study of the RC is a large undertaking. The entire protein-pigment complex consists of more than 10000 heavy atoms. Considering just the chromophores with hydrogens added, there are roughly 1100 atoms. We would like to be able to calculate the electronic properties of at least the chromophore aggregate of the RC. This system is too large to be effectively studied by current ab initio methods. Modelling the excited-state properties of the RC using the phenomenological coupled chromophore (or exciton) theory has clarified much about the excited states of the RC.[14-17] These models require a fitting of the basis of monomer excited states and their couplings to reproduce each system examined. While semiempirical methods do require parameterization based upon

† Present Address: Pacific Northwest Laboratory, Molecular Science Research Center, Richland, WA 99352.

(1) Feher, G.; Okamura, M. Y. In *The Photosynthetic Bacteria*; Clayton, R. K., Sistrom, W. R., Eds.; Plenum: New York, 1978; pp 349-386.
(2) Parson, W. W. *Annu. Rev. Biophys. Bioeng.* **1982**, *11*, 57.
(3) Parson, W. W. In *Photosynthesis*; Amesz, J., Ed.; Elsevier: Amsterdam, 1987; pp 43-61.
(4) Boxer, S. G. *Annu. Rev. Biophys. Biophys.* **1990**, *19*, 267.
(5) Friesner, R. A.; Won Y. *Biochim. Biophys. Acta* **1989**, *977*, 99.
(6) Kirmaier, C.; Holten, D. *Photosynth. Res.* **1987**, *13*, 225.
(7) Deisenhofer, J.; Epp, O.; Miki, K.; Huber, R.; Michel, H. *J. Mol. Biol.* **1984**, *180*, 385; *Nature (London)* **1985**, *318*, 618. Michel, H.; Epp, O.; Deisenhofer, *EMBO J.* **1986**, *5*, 2445. Deisenhofer, J.; Michel, H. In *The Photosynthetic Bacterial Reaction Center: Structure and Dynamics*; Breton, J., Vermeglio, A., Eds. (NATO ASI Series 149); Plenum: New York, 1988; pp 1-3.
(8) Chang, C. H.; Tiede, D.; Tang, J.; Smith, U.; Norris, J. R.; Shiffer, M. *FEBS Lett.* **1986**, *205*, 82.
(9) Yeates, T. O.; Komiya, H.; Chirino, A.; Raes, D. C.; Allen, J. P.; Feher, G. *Proc. Natl. Acad. Sci. U.S.A.* **1988**, *85*, 7993.
(10) Breton, J.; Martin, J.-L.; Petrich, J.; Migus, A.; Antonetti, A. *FEBS Lett.* **1986**, *209*, 37. Martin, J.-L.; Breton, J.; Hoff, A. J.; Migus, A.; Antonetti, A. *Proc. Natl. Acad. Sci. U.S.A.* **1986**, *83*, 957.
(11) Fleming, G. R.; Martin, J. L.; Breton, J. *Nature* **1988**, *12*, 190.
(12) Kirmaier, C.; Holten, D. *Proc. Natl. Acad. Sci. U.S.A.* **1990**, *87*, 3552.
(13) Kellog, E. C.; Kolaczkowski, S.; Wasielewski, M. R.; Tiede, D. M. *Photosynth. Res.* **1989**, *22*, 47.
(14) Warshel, A.; Parson, W. W. *J. Am. Chem. Soc.* **1987**, *109*, 6143. Parson, W. W.; Warshel, A. *J. Am. Chem. Soc.* **1987**, *109*, 6152.
(15) Eccles, J.; Honig, B.; Schulten, K. *Biophys. J.* **1988**, *53*, 137.
(16) Scherer, P. O. J.; Fischer, S. F. *Chem. Phys.* **1989**, *131*, 115.
(17) Knapp, E. W.; Scherer, P. O. J.; Fischer, S. F. *Biochim. Biophys. Acta* **1986**, *852*, 295.

0002-7863/91/1513-8210$02.50/0

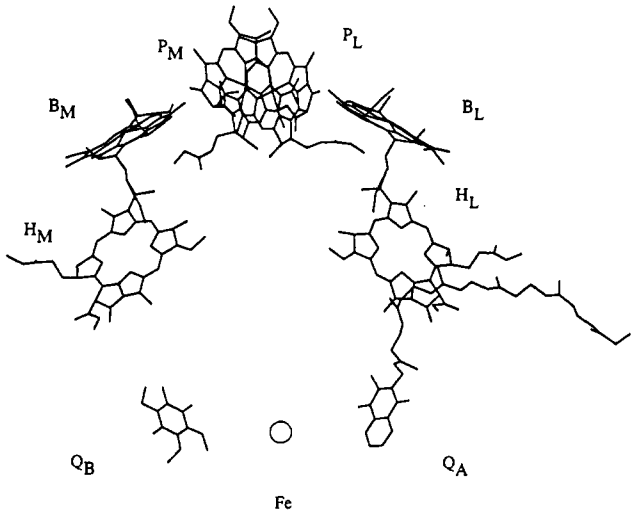

Figure 1. The chromophores of the photosynthetic reaction center of *Rps. viridis* from the 2.3-Å resolution X-ray structure. The protein subunits and the phytyl side chains for the BChl and BPh macrocycles are not shown. Abbreviations: P_M, P_L, M and L BChlb of the special pair; B_M, B_L, M and L auxiliary BChlb; H_M, H_L, M and L BPhb; Q_A = quinone A (menaquinone); Q_B = quinone (ubiquinone); Fe = nonheme iron atom. This figure is positioned with the periplasmic (extracellular) side at the top of the figure and the cytoplasmic (intracellular) side at the bottom of the figure.

experiment, there is no need to further reparameterize the method to each specific system studied. The intermediate neglect of differential overlap model for spectroscopy (INDO/S) has been directly parameterized at the singles excited configuration interaction level (CIS) to reproduce the spectra of benzene, pyridine, and the diazenes.[18] INDO calculations on photosynthetic reaction centers have been performed in the past by Scherer and Fischer,[16] but our procedures and results differ.

First, we would like to be able to reproduce the major features of the experimental optical absorption spectrum of intact RCs to assess the level of accuracy of our method. We will be particularly interested in reproducing the observed preference for the L branch over the M branch for the charge separation as well as being able to identify and order the important excited states that lead to charge separation between the chromophores. If these initial studies prove encouraging, we would feel confident to speculate on aspects of the detailed electronic structures of these systems that are not directly observed in experiment and that hamper our understanding of the mechanisms of photosynthetic charge transfer. In a subsequent work we would hope to use this method to calculate excited-state properties at various geometries in an unbiased fashion. In this way we could study the interaction of CT states with the low-lying excited states responsible for most of the absorption probability to better understand the internal conversion that drives the charge separation as well as the nature of the reaction coordinate. Here we make the reasonable assumption that the initial absorbing state has high transition probability, and as such is not the charge-transferring state itself. Such a state, with quite different structure than the ground (or "resting") state, would have low transition probability. After absorption, energy is transferred either directly, or indirectly, into the important CT state. This conversion appears without energy barrier. These assumptions are borne out by these calculations. A preliminary report of these findings has appeared.[19]

Methods

The calculations were performed with the intermediate neglect of differential overlap method (INDO) originally introduced by Pople and collaborators.[20] This method was later refined to accurately reproduce UV/vis spectra (INDO/S).[18] All SCF calculations were of the closed-shell restricted Hartree–Fock type (RHF). Calculated state dipole moments retained all one-center terms but omitted two-center contributions. Transition moments are calculated with the use of the dipole length operator in a similar fashion. Oscillator strengths calculated by CIS procedures are known to be overestimated by as much as a factor of 2. In general, this model reproduces the transition energies of the Q bands of the porphyrins but overestimates the higher energy B bands by 3000–5000 cm^{-1}.

Table I. Percent Localization of the MOs from the SCF of the RC Model

MO	energy, au	P_L	P_M	B_M	B_L	H_M	H_L
782	−0.000 816	29	70				
781	−0.003 308	70	29				
778	−0.007 819			85			
777	−0.010 372				96		
774	−0.031 468					100	
773	−0.035 711						100
772	−0.055 336	39	61				
771	−0.066 951			100			
770	−0.069 701				100		
769	−0.074 284	61	39				
768	−0.075 777					100	
767	−0.080 948						100
766[a]	−0.204 520	42	58				
765	−0.210 077	54	38	8			
764	−0.210 893	4	4	92			
763	−0.213 949				100		
762	−0.223 854					100	
761	−0.225 687						100
760	−0.237 483	60	39				
759	−0.252 014	38	61				
758	−0.259 362			99			
757	−0.259 928				99		
756	−0.265 058					100	
755	−0.268 632						100

[a] Highest occupied MO.

The coordinates of the heavy atoms of *Rps. viridis* were obtained from the X-ray data of Deisenhofer at 2.3-Å resolution.[7] Hydrogens were placed at standard distances and checked to ensure that no unacceptable steric interactions were generated. Except where stated, the heavy atom coordinates utilized were not altered or optimized further from the X-ray data.

Our initial model of the RC consisted of the four BChlb and the two BPhb chromophores shown in Figure 1. The phytyl side chains the BChl's and BPh's were truncated with a methyl group. We included the four histidine amino acid side chains that coordinate with the fifth position of the Mg atoms of the BChlb's. This RC model contains 536 atoms, 1436 basis functions (minimal valence basis), and 1532 electrons. Furthermore, to obtain a reasonable description of the excited states using a single-excitation configuration-interaction (CI) method requires the inclusion of a large number of configurations. To describe the low-energy excited states correctly, in a qualitative sense, would require at least 144 singly excited configurations, which assumes each chromophore contributes the four orbitals of Gouterman's model.[21] We find, in fact, that much larger calculations are required for the desired accuracy.

The calculations were performed with the quantum chemical program ARGUS[22] on the Cray YMP located at Florida State University, Tallahassee, FL. Each INDO/S SCF-CI calculation on the above RC model required roughly 1–2 h of single processor time.

Results and Discussion

Model Calculations. The SCF calculation suggests that the molecular orbitals (MOs) are largely localized to specific chromophores. The MOs of P are localized to P and demonstrate the supermolecule nature of the BChlb dimer.[23-25] The percent

(18) Ridley, J.; Zerner, M. *Theor. Chim. Acta (Berlin)* **1973**, *32*, 111; **1976**, *42*, 223. Zerner, M.; Loew, G.; Kirchner, R.; Mueller-Westerhoff, U. *J. Am. Chem. Soc.* **1980**, *102*, 589.
(19) Thompson, M. A.; Zerner, M. C. *J. Am. Chem. Soc.* **1990**, *112*, 7828.
(20) Pople, J. A.; Santry, D. P.; Segal, G. A. *J. Chem. Phys.* **1965**, *43*, S129. Pople, J. A.; Segal, G. A. *J. Chem. Phys.* **1965**, *43*, S136; **1966**, *44*, 3289. Santry, D. P.; Segal, G. A. *J. Chem. Phys.* **1967**, *47*, 158. Pople, J. A.; Beveridge, D. L.; Dobosh, P. A. *J. Chem. Phys.* **1967**, *47*, 2026.
(21) Gouterman, M. J. *J. Mol. Spectrosc.* **1961**, *6*, 138.
(22) ARGUS is a quantum chemical electronic structure program written by one of us (M.A.T.), implemented in the programming language C, and contains a vectorizable code for efficient performance on supercomputers.
(23) Källebring, B.; Larsson, S. *Chem. Phys. Lett.* **1987**, *138*, 76.
(24) Thompson, M. A.; Zerner, M. C. *J. Am. Chem. Soc.* **1988**, *110*, 606.
(25) Thompson, M. A.; Zerner, M. C.; Fajer, J. *J. Phys. Chem.* **1991**, *95*, 5693.

Table II. Coefficients for the Four- and Eight-Orbital Decomposition of Selected RC MOs[a]

MO	P	B_M	B_L	H_M	H_L
782	0.99 d_8				
781	0.99 d_7				
778		0.90 e_{gy}			
777			0.97 e_{gy}		
774				0.99 e_{gy}	
773					0.99 e_{gy}
772	−0.99 d_6				
771		0.99 e_{gx}			
770			−0.99 e_{gx}		
769	−0.99 d_5				
768				1.0 e_{gx}	
767					1.0 e_{gx}
766[b]	0.99 d_4				
765	−0.96 d_3				
764		0.96 a_{1u}			
763			−0.99 a_{1u}		
762				1.0 a_{1u}	
761					1.0 a_{1u}
760	−0.98 d_2				
759	0.97 d_1				
758		0.96 a_{2u}			
757			0.97 a_{2u}		
756				1.0 a_{2u}	
755					1.0 a_{2u}

[a] The symmetry labels for the monomer MOs are from Gouterman. Although D_{4h} symmetry labels do not strictly apply to bacteriochlorin derivatives, the D_{4h} symmetry labels are retained for convenience. The labels for the P MOs are described in the text. [b] Highest occupied MO.

localization of the 12 HOMOs and 12 LUMOs are shown in Table I. Not shown in Table I are MOs 776 and 780 which are localized on the histidine rings coordinated with the auxiliary BChlb, B_L and B_M, respectively. The Mg–N(hist) distance for these two structure are 2.09 Å and 2.17 Å, respectively. In spite of the presence of these two MOs among the lowest virtual MOs (as well as MOs 775 and 779), we observe that single excited configurations involving these MOs do not contribute significantly to the low-lying excited states of the RC model. Lengthening the Mg–N(hist) distances for these two structures did not greatly alter the results (data not shown). Note, in particular, that the highest lying occupied orbital is localized on P, while the lowest unoccupied orbital is localized on H_L. This order of molecular orbitals, by itself, might suggest flow of charge upon excitation in the observed direction along the L branch, an important point examined in some detail below.

In order to relate the MOs of the RC to specific MOs of the monomer subunits, we expand the RC MOs in a basis consisting of the MOs of P, B_L, B_M, H_L, and H_M.

$$\Psi_i^{RC} = \sum_\mu |\phi_\mu\rangle\langle\phi_\mu|\Psi_i^{RC}\rangle \qquad (1)$$

Here the coefficient that each basis MO contributes, $\langle\phi_\mu|\Psi_i^{RC}\rangle$, is the overlap of that MO with the RC MO. The MOs of the RC calculation were decomposed in this fashion using all MOs of the RC subunits as a basis. The results are given in Table II where we show the contribution of the basis MOs that make up the four-orbital model of Gouterman[21] for B_M, B_L, H_M, and H_L, and the eight-orbital model for P.[26] In this table, MOs labeled "d" are defined as shown in (2), where the coefficients depend

$$\begin{aligned}
d_8 &= (\sin\delta)e_{gy(L)} - (\cos\delta)e_{gy(M)}\\
d_7 &= (\cos\delta)e_{gy(L)} + (\sin\delta)e_{gy(M)}\\
d_6 &= (\sin\gamma)e_{gx(L)} - (\cos\gamma)e_{gx(M)}\\
d_5 &= (\cos\gamma)e_{gx(L)} + (\sin\gamma)e_{gx(M)}\\
d_4 &= (\sin\beta)a_{1u(L)} - (\cos\beta)a_{1u(M)}\\
d_3 &= (\cos\beta)a_{1u(L)} + (\sin\beta)a_{1u(M)}\\
d_2 &= (\sin\alpha)a_{2u(L)} - (\cos\alpha)a_{2u(M)}\\
d_1 &= (\cos\alpha)a_{2u(L)} + (\sin\alpha)a_{2u(M)}
\end{aligned} \qquad (2)$$

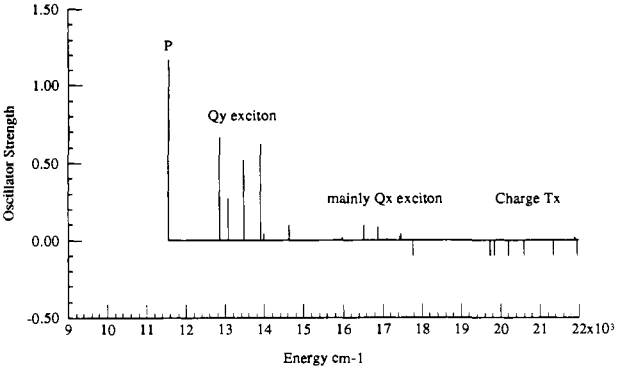

Figure 2. INDO/S calculated optical spectra of the RC from *Rps. viridis*. The calculation includes 1680 single excited configurations. The negative tics represent transitions with zero calculated oscillator strength.

Table III. INDO/S Excited States for the RC Model

state	energy (cm^{-1})	oscill. str.	comment
1	11550	1.17	P Q_{y1}
2	12849	0.67	P Q_{y2}
3	13069	0.27	mixed Q_y states of mainly B_L, B_M, H_L, H_M
4	13473	0.52	
5	13898	0.62	
6	13981	0.04	
7	14628	0.10	P Q_y
8	15976	0.02	mainly P Q_{y3}
9	16518	0.10	mix of P Q_y ... and P Q_x
10	16877	0.08	
11	17099	0.01	H_L Q_x
12	17306	0.00	$B_LH_L \rightarrow B_L^+H_L^-$
13	17435	0.03	mix of B_M Q_x ... and H_M Q_x
14	17460	0.01	
15	17461	0.04	B_L Q_x
16	17765	0.00	$B_MH_M \rightarrow B_M^+H_M^-$
17	17809	0.00	$PB_M \rightarrow P^-B_M^+$
18	17843	0.00	$PB_L \rightarrow P^+B_L^-$
19	19728	0.00	$PH_L \rightarrow P^+H_L^-$
20	19836	0.00	$PB_L \rightarrow P^+B_L^-$
21	20193	0.00	$PB_M \rightarrow P^+B_M^-$
22	20589	0.00	$PH_M \rightarrow P^+H_M^-$

on the specific geometry of the dimer. For example, the coefficients would equal $1/\sqrt{2}$ for a symmetric dimer spaced far enough apart to be weakly interacting.[26] The dimer labels d_1 – d_8 were developed previously in a study of Mg–bacteriochlorin model dimers.[26] The D_{4h} labels have been retained for convenience, as is conventional in porphyrin chemistry, even though these molecules possess no particular symmetry. The RC MOs we show are those that dominate the low-energy calculated spectra of the RC model and, as well, are described by the four- and eight-orbital models for the monomer and dimer, respectively.

A single excitation CI was performed to obtain a description of the optical spectra of the RC. The MO active space was chosen to balance the number of MOs for symmetry related chromophores in both the L and M branches (Figure 1) and include at least the 12 occupied and 12 virtual MOs required to fulfill the four- and eight-orbital models of the chromophores. Thus, we included all single excited configurations from the 40 highest occupied MOs into the 42 lowest virtual MOs. This resulted in 1680 excited configurations. The calculated optical spectrum for energies up to 22000 cm^{-1} is shown in Figure 2. We give a description of select CI states in Table III.

The two lowest energy transitions, states 1 and 2, correspond to the lower and upper exciton states of the Q_y bands of P, respectively.[14,15,27] The assignment of these states is based on the

(26) Thompson, M. A.; Zerner, M. C.; Fajer, J. *J. Phys. Chem.* **1990**, *94*, 3820.

(27) Breton, J. *Biochim. Biophys. Acta* **1985**, *810*, 235. Breton, J. In *The Photosynthetic Bacterial Reaction Center: Structure and Dynamics*; Breton, J., Vermeglio, A., Eds. (NATO ASI Series 149); Plenum: New York, 1988; pp 59–69.

Table IV. INDO/S Calculated Energies and Dipole Moment Differences with the Ground State for Q_{y1} and CT States from the RC Model

		"gas-phase" calculation		Solvent calculation[b]	
	state[c]	energy (cm^{-1})	$\|\Delta\mu\|$[a] (vector)	energy (cm^{-1})	$\|\Delta\mu\|$
1	Q_{y1}	11550	4.6 (−2.2, −3.8, 1.6)	11461	4.6
12	$B_LH_L \rightarrow B_L^+H_L^-$	17306	48.1 (−9.9, −41.7, 21.9)	13948	47.1
16	$B_MH_M \rightarrow B_M^+H_M^-$	17765	48.1 (−38.8, −24.5, 14.32)	14406	47.1
17	$PB_M \rightarrow P^-B_M^+$	17809	45.3 (27.6, −22.0, −28.3)	16510	45.4
18	$PB_L \rightarrow P^-B_L^+$	17843	41.4 (−11.0, 34.0, 20.9)	16577	41.5
19	$PH_L \rightarrow P^+H_L^-$	19728	78.9 (−12.3, −77.9, −2.0)	12609	75.0
20	$PB_L \rightarrow P^+B_L^-$	19836	49.9 (0.5, −48.7, 10.8)	16598	46.1
21	$PB_M \rightarrow P^+B_M^-$	20193	55.5 (−23.9, 14.4, 48.0)	16713	48.4
22	$PH_M \rightarrow P^+H_M^-$	20589	76.9 (−51.6, −15.2, 55.0)	13496	74.8

[a] The calculated dipole moment of the excited state minus the ground state (D). This is followed by ($\Delta\mu_x$, $\Delta\mu_y$, $\Delta\mu_z$). [b] $\epsilon = 2.023$, $\eta = 1.4266$, and $a_0 = 10.6$ Å (see text). [c] The numbering of states is the same as in Table III.

phase and magnitude of their major contributing configurations and the description of the MOs given in Table II. The labels Q_{y1} and Q_{y2} were developed previously[25,26] and would correspond to the alternate usage of $P^*_{(-)}$ and $P^*_{(+)}$, respectively.[14,15,27] There has been some discussion in the literature concerning the placement of the upper exciton component of P.[5,14-16,27] Experimentally, a shoulder located at about 850 nm (11765 cm^{-1}, about 1500 cm^{-1} above $P^*_{(-)}$; see later discussion), which is on the low-energy side of the more intense absorption of the Q_y bands of B_L and B_M, is observed. In their coupled chromophore treatment of the RC, Warshel and Parson attribute this shoulder to B_L and B_M and place the $P^*_{(+)}$ band at 812 nm with significant mixing with the Q_y states of the other four chromophores in the RC.[14] Alternatively, in their exciton model analysis of the RC, Eccles, Honig, and Schulten concluded that placement of the upper exciton component of P at 850 cm^{-1} was required to successfully reproduce the optical, LD, and CD spectrum of the RC.[15] Inasmuch as Q_{y2} is the second lowest excited state in our calculation, and lies 1300 cm^{-1} above Q_{y1}, our results are consistent with the identity of the upper exciton component of P with the shoulder at 850 nm.

We now turn to calculations of linear dichroism (LD). We define a pseudo-C_2 symmetry axis for this RC model that extends from the Fe atom to the average coordinates of the Mg atoms of P. The angle of the transition moments for the excited states with this axis can be compared to experimental LD results.[27] We calculate this angle for Q_{y1} and Q_{y2} as 86.3° and 10.1°, respectively. This compares to the corresponding experimental LD values given by Breton as 90° and 30°.[27] We note here that there is some uncertainty in the value of 30° for Q_{y2} reported by Breton.[27] Calculations assuming only exciton coupling within the BChlb monomers of P give values of 88° and 10° for Q_{y1}, and Q_{y2}, respectively.[27] We calculate the Q_{y1}–Q_{y2} splitting to be 1300 cm^{-1}, which compares to a calculated value of 1509 cm^{-1} for P calculated separately with its histidine ligands,[25] and to the experimental splitting of ~1350–1700 cm^{-1}, depending upon temperature.[5,6,28] The CI used in the calculation of the RC model contained 17 occupied and 10 virtual MOs localized on P. This gives 170 configurations specific to the active space of P. We do not span as large an active space for P in these RC calculations as we can afford to do in the calculations done on P alone.[25] Thus we observe that the calculated energies of Q_{y1} and Q_{y2} for the RC model (11550 cm^{-1} and 12849 cm^{-1}, respectively) are blue shifted compared to their calculated transition energies for P with its two ligating histidines (10982 cm^{-1} and 12490 cm^{-1}, respectively).[25] This represents a blue shift of 568 cm^{-1} and 359 cm^{-1} for Q_{y1} and Q_{y2}, respectively, between these two calculations. This might be considered as an error caused by our inability to perform a sufficiently large CI to reproduce the results of our calculations on isolated chromophores and the dimer. Although this error seems small, we remark that the splitting between Q_{y1} and Q_{y2} has decreased from 1509 cm^{-1} for P alone, to 1299 cm^{-1} in the RC model. This smaller splitting is attributed in part to the increased mixing of Q_{y2} with the Q_y bands from the other BChl and BPh monomers in the RC model which tends to retard the blue shift of Q_{y2} in this RC model (about 25% of Q_{y2} is from configurations specific to H_L, B_M, and B_L (data not shown)). A larger active space in the CI, specific to P, should red shift states Q_{y1} and Q_{y2} and may lessen the Q_y contributions to Q_{y2} from the other chromophores in the RC.

To the high-energy side of Q_{y2} are four states ranging in transition energy from 13069 cm^{-1} to 13981 cm^{-1}. These states are dominated by the Q_y states of the four monomeric chromophores in the RC model with some small contribution from the Q_y state of P. In accord with experiment, we calculate the Q_y exciton states of these branch chromophores just to the high-energy side of Q_{y2}. We further observe that these four excited states are calculated within 1000 cm^{-1} of one another, and their detailed mixing is a sensitive function of their nearly degenerate energies before interaction and the size of their coupling.[29] Regardless, our calculations yield four Q_y-based states with significant mixing between the Q_y transitions of B_L, B_M, H_L, and H_M, making it difficult to assign them to specific chromophores as done experimentally.[5,6,27,28] From LD experiments, the angle between the RC C_2 axis and the Q_y transitions for B_M, B_L, H_M, and H_L have been determined to be roughly 70°, 70°, 40°, and 40°, respectively.[27] We calculate the Q_y LD angle for the monomers (calculated separately) as 68°, 65°, 38°, and 34° for B_M, B_L, H_M, and H_L, respectively. The calculated angles for states 3–6 from Table III for the RC are 67°, 52°, 66°, and 73°, respectively. The experimental values bracket our values and appear to reflect an averaging of the branch chromophores' Q_y angles consistent with the strong mixing we observe in our calculations.

The strong overlap and mixing of the Q_{y2} transition of P and the Q_y transitions of the other chromophores of the RC could have important consequences in the energy-transfer process from the antenna to B (or H) into the special pair. The implication is that energy from the antenna enters through the Q_y states of B or H and transfers to Q_{y2}, which then relaxes to Q_{y1}.[30]

Several states are dominated by electron transfer between chromophores and we label these as CT states (Table III). The energies and difference in state dipole moments for these states with the ground state are given in Table IV. We have found that these states are usually dominated by one or two configurations representing inter-chromophore excitations. As such, we observe that the placement of these CT transitions in our calculations is largely insensitive to the size of the active space in the CI. The energies of these CT states can be estimated from the SCF results and knowledge of the RC geometry by the formula

$$E_{CT} \simeq \epsilon_{virt}^{B} - \epsilon_{occ}^{A} - J_{occ,virt} + 2K_{occ,virt} \qquad (3a)$$

which is merely the difference in orbital energies on chromophores A and B offset by the Coulomb (J) and exchange (K) interaction between the separated charge. Ignoring exchange, which should be small for chromophores that are well separated, and assuming $J_{occ,virt} = R^{-1}$, the Coulomb repulsion between cation and anion,

(28) Vermeglio, A.; Paillotin, G. *Biochim. Biophys. Acta* **1982**, *681*, 32.

(29) This parameterization of the INDO/S method is based on a single excitation configuration interaction and utilizes the dipole-length operator for calculating transition moments. It is commonly observed that CI-singles methods such as this overestimate the calculated oscillator strength and, as a consequence, tend to overestimate excitonic couplings of nearly degenerate localized excited states.

(30) We are grateful to G. Fleming (Chicago) for pointing this out to us.

we can estimate the E_{CT} for ($PH_L \rightarrow P^+H_L^-$) as

$$E_{CT} = EA^B - IP^A - 1/R_{AB} \quad (3b)$$

where we have used Koopmans' approximation that the negative of an occupied orbital energy estimates an ionization potential (IP) and an unoccupied orbital energy estimates an electron affinity (EA). Using the energies of the HOMO and LUMO from our RC calculation (Table I) and the center-to-center distance of about 17 Å between P and H_L, we obtain a value of about 20 290 cm^{-1} compared to 19 728 cm^{-1} from our CI calculation (Tables III and IV).

The large values of $|\Delta\mu|$ and their vectorial direction are consistent with the CT character of these states between the relevant chromophores and will prove important in our later discussions. Note that states $PH_L \rightarrow P^+H_L^-$ and $PH_M \rightarrow P^+H_M^-$ have the largest values of $|\Delta\mu|$, being 78.9 and 76.9 D, respectively.[31] These dipole magnitudes are roughly 1.5–2.0 times as large as the other CT states which is indicative of the larger distance involved in the charge separation relative to the other states. The asymmetry of the RC model is apparent in the relative ordering of analogous CT states involving the L- and M-branch chromophores. Charge transfer from P to the auxiliary BChlb favors the L versus the M branch by 356 cm^{-1} (states 20 and 21), while CT from P to BPhb energetically favors the L versus the M branch by 860 cm^{-1} (states 19 and 22). As well, CT states from the corresponding BChlb to BPhb for the L versus the M branch favors the L branch by 460 cm^{-1} (states 12 and 16). In both the RC calculations and in calculations on H_L and H_M done separately, we observe that the HOMO–LUMO gap is smaller for H_L and the LUMO energy of H_L lies below that of H_M. Thus we calculate the Q_y band of H_L lower in energy than H_M (12 345 cm^{-1} and 12 903 cm^{-1}, respectively). This compares with the experimental values reported by Breton as ~12 422 cm^{-1} and 12 658 cm^{-1} for the Q_y bands of H_L and H_M, respectively, in the RC at 10 K.[27] This, in part, explains the asymmetry of the L versus the M branch that places the $PH_L \rightarrow P^+H_L^-$ CT transition roughly 860 cm^{-1} lower in energy than $PH_M \rightarrow P^+H_M^-$. Consideration of specific amino acids close to H_L or H_M could affect this ordering as could experimental error in the X-ray crystal coordinates.

For these calculations, the vertical energy separation between Q_{yl} and the CT states ranges from about 6000 to 9000 cm^{-1}. We would expect, for an activationless or pseudoactivationless primary electron transfer, that the relevant CT states would be accessible to the lowest excited state by a much smaller energy gap than is demonstrated by our calculation. The expected energy gap should be the order of a vibrational quanta of energy (no greater than 1000–2000 cm^{-1}). Also, the results give $B_LH_L \rightarrow B_L^+H_L^-$ as the lowest accessible CT state, almost 2400 cm^{-1} lower in energy than $PB_L \rightarrow P^+B_L^-$ and $PH_L \rightarrow P^+H_L^-$. Even assuming that the energies of these CT states are strongly affected by small geometric changes, it is difficult to envision that these changes would reorder the CT states and place them sufficiently close in energy to Q_{yl} for the necessary internal conversion to occur.

Including the Protein as a Polarizable Medium. The chromophores of the RC are imbedded in a protein complex, which itself is embedded within the cell membrane. There are several nearby amino acids that exhibit specific interactions with the chromophores which may affect the photophysical and dynamic properties of the RC.[7-9,32,33] In addition, the remainder of the surrounding protein is a polarizable media. Because of the large change in dipole moment of the CT states, we should address the effects of a polarizable medium on the energy and ordering of these states. We include the effects of the protein as a polarizable solvent using the self-consistent reaction field (SCRF) method first developed by Tapia and Goscinski[34] and later refined by Karelson and Zerner for spectroscopy.[35] This model treats the solvent as an isotropic polarizable medium. The solute Hamiltonian, H_0, is modified by a perturbation due to the solvent, H_1.

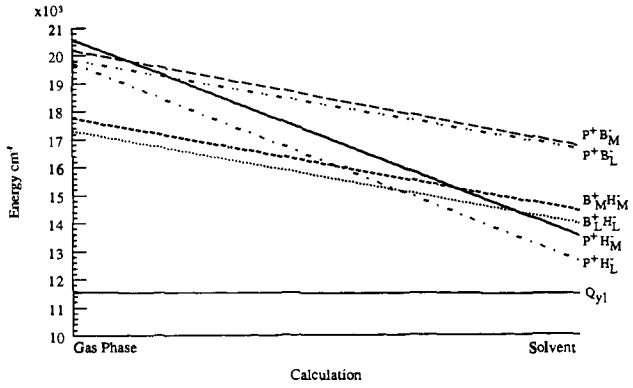

Figure 3. Energies of CT states and Q_{yl} in the absence and presence of the solvent model. The abscissa is arbitrary, the two end points representing the gas-phase calculation ($\epsilon = 1$) and the protein surroundings ($\epsilon = 2$).

$$H_{rf} = H_0 + H_1 \quad (4)$$

A set of modified Fock equations that incorporates this solvent perturbation is derived.[34,35]

$$f = f_0 - g\vec{\mu}\cdot\langle\vec{\mu}\rangle \quad (5)$$

$$g = \frac{1}{a_0^3}\frac{\epsilon - 1}{2\epsilon + 1} \quad (6)$$

where ϵ is the solvent dielectric constant, μ the dipole moment operator, and a_0 the effective radius of the solvent cavity. The second term in eq 5 represents the reaction field at the solute molecule generated by the solvent. The SCRF equations are solved iteratively in the usual fashion until an SCF is achieved. A single excited CI is performed from the single determinant SCRF ground state. The solvent energy correction to the excited states is given as

$$\Delta E_{CI} = -\frac{1}{a_0^3}\left(\frac{\eta^2 - 1}{2\eta^2 + 1}\right)(\langle\vec{\mu}^*\rangle - \langle\vec{\mu}\rangle)\cdot\langle\vec{\mu}^*\rangle \quad (7)$$

and accounts for the fact that only the electronic polarization can respond during the absorption process. In eq 7 η represents the solvent refractive index and $\langle\vec{\mu}^*\rangle$ the dipole moment of the solute excited state. The reaction field model assumes a spherical solvent cavity with radius a_0. Our choice of a value for a_0 is based the mass density of the RC model:

$$^4/_3\pi a_0^3 = M/\rho \quad (8)$$

where M is the molar mass and ρ is the mass density of the RC model. We used a value of 1.336 g/cm^3 for ρ which is the mass density of porphin. This formulation gives an effective cavity radius of 10.6 Å. We modelled the protein as a solvent having the bulk properties of cyclohexane ($\epsilon = 2.023$ and $\eta = 1.4266$). We recognize that there are shortcomings in this model and that specific interactions that might be important are not included.

(31) The fact that the dipole moment of the $P^+H_L^-$ is greater than that of $P^+H_M^-$ might suggest that P has greater formal separation from H_L than to H_M. This is counter to suggestions made that H_L is closer to P, on average, and this explains, in part, the more effective transfer rate down the L side; see, for example, ref 32, and Plato, M., et al. *J. Am. Chem. Soc.* **1988**, *110*, 7279. Of course, the details of the charge transfer do not depend on average separation, but detailed contacts.

(32) Parson, W. W.; Chu, Z.; Warshel, A. *Biochim. Biophys. Acta* **1990**, *1017*, 251.

(33) Tiede, D. M.; Budil, D. E.; Tang, J.; El-Kabbani, O.; Norris, J. R.; Chang, C.-H.; Schiffer, M. In *The Photosynthetic Bacterial Reaction Center Structure and Dynamics*; Breton, J., Vermeglio, A., Eds. (NATO ASI Series 149); Plenum: New York, 1988; pp 13–20.

(34) Tapia, O.; Goscinski, O. *Mol. Phys.* **1975**, *29*, 1653.

(35) Karelson, M. M.; Katritzky, A. R.; Szafran, M.; Zerner, M. C. *J. Chem. Soc., Perkin Trans.* **1990**, *2*, 195; *J. Org. Chem.* **1989**, *54*, 6030. Karelson, M. M.; Tamm, T.; Katritzky, A. R.; Cato, S. J.; Zerner, M. C. *Tetrahedron Comput. Methodol.* **1989**, *2*, 295. Karelson, M. M.; Zerner, M. C. *J. Am. Chem. Soc.* **1990**, *112*, 9405. Karelson, M. M.; Zerner, M. C. In preparation.

On the other hand, it is reasonable to expect that a dipole moment change of nearly 80 D will certainly have a noticeable effect on the surrounding protein.

The results of the calculated optical spectra of our RC model employing the above solvent model showed relatively little change to the local exciton-like excited states. This is what we would expect for states exhibiting small dipole changes. The Q_{y1} state does exhibit a small amount of internal CT character between the BChlb monomers,[25] and we do observe a shift in energy from 11 550 cm^{-1} to 11 461 cm^{-1} between the "gas phase" and solvent calculations, respectively. However, we observe large changes in the energies and the relative ordering of the CT states. Table IV and Figure 3 compare the results for the CT states in the gas phase and the solvent calculation. Note that the CT states are all lowered in energy relative to the gas-phase calculation and their relative ordering is changed. In the SCRF case, we calculate that $PH_L \rightarrow P^+H_L^-$ is now within about 1200 cm^{-1} of Q_{y1}. Furthermore, CT from P to both the BPhb chromophores is considerably lower in energy than those from P to the auxiliary BChlb chromophores. This concurs with the lack of an experimentally observed intermediate involving either B_L^+ or B_L^- in picosecond and subpicosecond experiments.[10,11] The splitting between $PH_L \rightarrow P^+H_L^-$ and $PB_L \rightarrow P^+B_L^-$ is about 4000 cm^{-1}, whereas the splitting between $PH_L \rightarrow P^+H_L^-$ and $B_LH_L \rightarrow B_L^+H_L^-$ is about 1300 cm^{-1}. Our results suggest against an explicit intermediate involving B_L[36] although we cannot rule out a specific interaction with B_L that we have not included.

In our previous work on the dimer, we not only examine the bare dimer, but also the dimer in the field of 38 amino acids within a radius of 12 Å of the center of the dimer.[25] The inclusion of these specific amino acids has very little effect on the transition energies and nature of the calculated excited states. A somewhat greater charge separation is noted in P* (0.07 e L → M versus 0.03 e L → M) when the neighboring amino acids are included and the calculated Stark angle does rotate into better agreement with experiment.[25] That study and the present one, however, do not ensure that important residues we have neglected will not have a measurable influence on the results we report here.

Conclusions

We have presented quantum chemical calculations that reproduce the major characteristics of the optical spectrum of the RC. Consistent with experiment, the two lowest excited states of the RC (Q_{y1} and Q_{y2}) are attributed to the BChlb dimer, P, and consist mainly of the lower and upper exciton components of the constituent monomers of P, respectively. At higher energies we predict four bands associated with the Q_y states of the remaining RC chromophores (states 3–6, Table III). Our predicted mixing among these states prevents an assignment to individual chromophores[29] as has been done experimentally.[5,6,27,28] However, this strong mixing does give an explanation for the rapid energy transfer observed between the other chromophores of the RC and P.[30]

The importance of the presence of a polarizable protein in stabilizing states with large charge separation is clearly demonstrated by modelling this effect through the use of a self-consistent reaction field model. After consideration of the dielectric relaxation of the protein, the $PH_L \rightarrow P^+H_L^-$ excited state is calculated to lie ~1200 cm^{-1} above the lowest absorbing state, Q_{y1}. This number is small enough to lead to pseudo-activationless internal conversion along a RC vibrational mode, or even through further reorientational relaxation of the protein. We estimate that, even with dielectric relaxation, the $PB_L \rightarrow P^+B_L^-$ state lies some 4000 cm^{-1} above $PH_L \rightarrow P^+H_L^-$ and is thus unlikely to contribute in a direct fashion to the charge separation *in the absence of a specific interaction that we may not have considered.*[32,33,36] This still leaves as a mystery how charge can be separated so quickly over such a large distance without invoking the auxiliary BChlb's. The reason that nearly degenerate charge-transfer excitations from P to the BChlb and BPhb (Table IV) are well separated in the presence of a polarizable protein is well understood by the very different sizes of their resultant dipole moments.

At all levels of calculation, the states that transfer charge from P to the L side of the RC are lower in energy than those to the M side. In our most realistic model calculations (with the protein modelled as a polarizable medium), the $PH_L \rightarrow P^+H_L^-$ state lies about 880 cm^{-1} below $PH_M \rightarrow P^+H_M^-$. Assuming entropic contributions to both process are roughly the same and room-temperature conditions, simple thermodynamics leads to about a 70:1 bias for charge transfer to occur along the L branch, to be compared with estimates ranging from 100:1 to 200:1 experimentally.[37] We recognize that for this simple analysis to have relevance in the context of the observed charge-transfer process we must assume that the electronic coupling matrix elements between P* and $P^+H_L^-$ and between P* and $P^+H_M^-$ are similar, and thus populate both $P^+H_L^-$ and $P^+H_M^-$ according to a Boltzmann distribution. Arguments based upon geometry that suggest $|\langle P^*|V|P^+H_L^-\rangle| > |\langle P^*|V|P^+H_M^-\rangle|$ need not be made.[30-32]

The asymmetry that we observe in these calculations, L versus M, is clearly a consequence of the distortions from C_2 symmetry shown in the coordinates of the *Rps. viridis* X-ray crystal structure, which, in turn, is a result of the protein scaffolding.[31,38-40] No specific interactions with the protein were required to cause this. Since this structure yields L side charge-receiving states lower in energy than M side, changes to P, for example, "heterodimers" consisting of BChl–BPh,[41-44] should have only small effects on the direction of charge transfer, providing P continues to behave as a supermolecule, and, of course, its initial excited state possesses enough energy to drive charge separation. This argues against any charge asymmetry developing in P* as being crucial to determining the directionality of the initial charge separation.[25]

It would be interesting to examine what asymmetry of the RC causes this effect. Such a study would require that the orientation of each chromophore be modified via altered chromophore–amino acid interactions in genetically engineered RCs. Our calculations are sensitive to macrocycle distortions caused by the protein scaffold. Also, potentially important in affecting the charge receiving states could be the presence of charged or polarizable residues that could also be constructed via genetic techniques. Of specific interest would be the presence of positively charged or dipolar residues in the vicinity of B_L. This may cause sufficient lowering of the $PB_L \rightarrow P^+B_L^-$ CT state that could allow for the observation of $P^+B_L^-$ as an explicit intermediate in the initial CT process.

Acknowledgment. This work was supported, in part, through grants from Eastman Kodak Co. and the Office of Naval Research at the University of Florida. M.A.T. acknowledges the support of the National Science Foundation and Shell Oil for predoctoral fellowships. We gratefully acknowledge stimulating discussions with Jack Fajer (Brookhaven National Laboratory).

(36) Holzapfel, W.; Finkele, U.; Kaiser, W.; Oesterhelt, D.; Scheer, H.; Stilz, H. U.; Zinth, W. *Proc. Natl. Acad. Sci. U.S.A.* **1990**, *87*, 5168.

(37) Kellog, E. C.; Kolaczkowski, S.; Wasielewski, M. R.; Tiede, D. M. *Photosynth. Res.* **1989**, *22*, 47.

(38) Gudowska-Nowak, E.; Newton, M. D.; Fajer, J. *J. Phys. Chem.* **1990**, *94*, 5795.

(39) Barkigia, K. M.; Chantranupong, L.; Smith, K. M.; Fajer, J. *J. Am. Chem. Soc.* **1988**, *110*, 7566.

(40) Forman, A.; Renner, M. W.; Fujita, E.; Barkigia, K. M.; Evans, M. C. W.; Smith, K. M.; Fajer, J. *Isr. J. Chem.* **1989**, *29*, 57.

(41) Kirmaier, C.; Holten, D.; Bylina, E. J.; Youvan, D. C. *Proc. Natl. Acad. Sci. U.S.A.* **1988**, *85*, 7562. Bylina, E. J.; Youvan, D. C. *Proc. Natl. Acad. Sci. U.S.A.* **1988**, *85*, 7226. Kirmaier, C.; Bylina, E. J.; Youvan, D. C.; Holten, D. *Chem. Phys. Lett.* **1989**, *159*, 251.

(42) McDowell, L. M.; Kirmaier, C.; Holten, D. *Biochim. Biophys. Acta*, in press; *J. Phys. Chem.*, in press.

(43) DiMagno, T. J.; Bylina, E. J.; Angerhofer, A.; Youvan, D. C.; Norris, J. R. *Biochemistry* **1990**, *29*, 899.

(44) Hammes, S. L.; Mazzola, L.; Boxer, S. G.; Gaul, D. F.; Schenck, C. C. *Proc. Natl. Acad. Sci. U.S.A.* **1990**, *87*, 5682.